Hydroxyl radical reactions with halogenated ethanols in aqueous solution: Kinetics and thermochemistry

ARTICLE *in* INTERNATIONAL JOURNAL OF CHEMICAL KINETICS · APRIL 2008

Impact Factor: 1.52 · DOI: 10.1002/kin.20301

Hydroxyl Radical Reactions with Halogenated Ethanols in Aqueous Solution: Kinetics and Thermochemistry

I. MOROZOV,[1] S. GLIGOROVSKI,[2] P. BARZAGHI,[2] D. HOFFMANN,[2] Y. G. LAZAROU,[3] E. VASILIEV,[1] H. HERRMANN[2]

[1]*Semenov Institute of Chemical Physics* RAS, *Kosygin Str.* 4, 119991 *Moscow, Russia*
[2]*Leibniz-Institut für Troposphärenforschung, Permoserstraße* 15, 04318 *Leipzig, Germany*
[3]*Institute of Physical Chemistry, National Centre of Scientific Research "Demokritos," Aghia Paraskevi, Attiki* GR-153 10, *Greece*

Received 21 December 2006; revised 21 May 2007, 23 October 2007; accepted 24 October 2007

DOI 10.1002/kin.20301
Published online in Wiley InterScience (www.interscience.wiley.com).

ABSTRACT: Laser flash photolysis combined with competition kinetics with SCN^- as the reference substance has been used to determine the rate constants of OH radicals with three fluorinated and three chlorinated ethanols in water as a function of temperature. The following Arrhenius expressions have been obtained for the reactions of OH radicals with (1) 2-fluoroethanol, $k_1(T) = (5.7 \pm 0.8) \times 10^{11}$ exp((−2047 ± 1202)/T) M^{-1} s^{-1}, (2) 2,2-difluoroethanol, $k_2(T) = (4.5 \pm 0.5) \times 10^9$ exp((−855 ± 796)/T) M^{-1} s^{-1}, (3) 2,2,2-trifluoroethanol, $k_3(T) = (2.0 \pm 0.1) \times 10^{11}$ exp((−2400 ± 790)/T) M^{-1} s^{-1}, (4) 2-chloroethanol, $k_4(T) = (3.0 \pm 0.2) \times 10^{10}$ exp((−1067 ± 440)/T) M^{-1} s^{-1}, (5) 2,

Correspondence to: H. Herrmann; e-mail: herrmann@tropos.de.
Present address of S. Gligorovski: Laboratoire Chimie et Environnement Université de Provence, Case courrier 29, 3 place Victor Hugo, 13331 Marseille Cedex 03, France.

Contract grant sponsor: European Commission, under the project "Impact of Fluorinated Alcohols and Ethers on the Environment (IAFAEE)."
Contract grant number: EVK2-CT-1999-00009.
Contract grant sponsor: North Atlantic Treaty Organization.
Contract grant number: CLG 983035.
Contract grant sponsor: International Association for the promotion of cooperation with scientists from the New Independent States of the former Soviet Union (NIS).
Contract grant number: 03-51-56-98.
Contract grant sponsor: Russian Foundation for Basis Research.
Contract grant numbers: 06-05-64646, 06-03-32836.

2-dichloroethanol, $k_5(T) = (2.1 \pm 0.2) \times 10^{10} \exp((-1179 \pm 517)/T)$ M^{-1} s^{-1}, and (6) 2,2,2-trichloroethanol, $k_6(T) = (1.6 \pm 0.1) \times 10^{10} \exp((-1237 \pm 550)/T)$ M^{-1} s^{-1}. All experiments were carried out at temperatures between 288 and 328 K and at pH = 5.5–6.5. This set of compounds has been chosen for a detailed study because of their possible environmental impact as alternatives to chlorofluorocarbon and hydrogen-containing chlorofluorocarbon compounds in the case of the fluorinated alcohols and due to the demonstrated toxicity when chlorinated alcohols are considered. The observed rate constants and derived activation energies of the reactions are correlated with the corresponding bond dissociation energy (BDE) and ionization potential (IP), where the BDEs and IPs of the chlorinated ethanols have been calculated using quantum mechanical calculations. The errors stated in this study are statistical errors for a confidence interval of 95%. © 2008 Wiley Periodicals, Inc. Int J Chem Kinet 40: 174–188, 2008

INTRODUCTION

The ability of a chemical compound to create a greenhouse effect in the atmosphere is caused by shielding radiation being emitted from the earth surface in the atmosphere. Potential greenhouse gases may be characterized by their greenhouse warming potential (GWP) with the GWP being the ratio of the warming caused by a substance to the warming caused by a similar mass of carbon dioxide [1].

Because of their capacity to destroy the ozone layer and having high GWPs, various classes of industrially produced halocarbon compounds such as chlorofluorocarbon compounds (CFCs) and hydrogen-containing chlorofluorocarbon compounds (HCFCs) are subject to international regulations and have been phased out from industrial production to a large extent [1]. Therefore, the substitution of such compounds is an industrial and environmental issue of huge importance.

Different approaches have been chosen to develop compounds as alternatives to CFCs and HCFCs with reduced effects on the environment.

Halogenated ethanols (HEs) have been suggested as such alternative compounds [2]. The atmospheric lifetime and the degradation pathways of such alternative compounds must be established to assess the possible impact of the industrial application of HEs to the atmosphere.

One of the ways that has been chosen is the use of fluorine as the only substituent in the organic compound since fluorocarbon oxidation products do not seem to be able to catalyze stratospheric ozone depletion. Thus, fluorinated alcohols (FAs) have received attention as potential alternative compounds [1], and a recent study of Sellevåg et al. [2] investigated the gas-phase reactivity of 2-fluoroethanol, 2,2-difluoroethanol, and 2,2,2-trifluoroethanol.

Because of their solubility [3,4], significant concentrations of FAs could be expected to be transferred to the atmospheric aqueous phases. Reactive uptake into cloud particles has been proposed as a possible significant loss process for trifluoromethanol under tropospheric conditions [5]. Thus, the most likely sinks for halogenated alcohols are deposition or chemical conversion processes in the aqueous phase where an important first step of halogenated ethanols atmospheric degradation could proceed by reaction with the OH radical in aqueous solution.

As another family of compounds, chlorinated alcohols (ChAs) attract interest as compounds for a comparison of their reactivity toward OH radical with that of FAs of similar structure. ChAs are used in a wide variety of industrial applications as solvents, additives, and intermediates in chemical synthesis. They are also generated by bacterial biotransformation or hydrolysis of widely employed halogenated ethanes [6,7]. In particular, $CHCl_2CH_2OH$ may be also generated by the hydrolysis of the pesticide dichlorvos [8]. Generally, chloroethanols are considered to be toxic to marine and terrestrial animals [9,10]. Furthermore, the natural formation of organohalogen compounds has been suggested to contribute to the atmospheric budget [11]. In fact, the halogenation of hydrocarbons is well documented for nearly all-natural environments where the oceans represent the strongest production source of organohalogen of biogenic origin. Most of the identified compounds in the maritime environment are chloro-substituted hydrocarbons [12], whereas in continental areas the bromine-substituted organics are formed. Biogenic formation of fluoro-organic compounds is of minor importance. Organofluorine metabolites have been found in bacteria, fungi, and higher plants [13–15].

Several experimental studies [2,16–19] have been published on the gas-phase reactivity of OH radicals toward halogenated alcohols, whereas much less information is available for possible aqueous-phase degradation reactions.

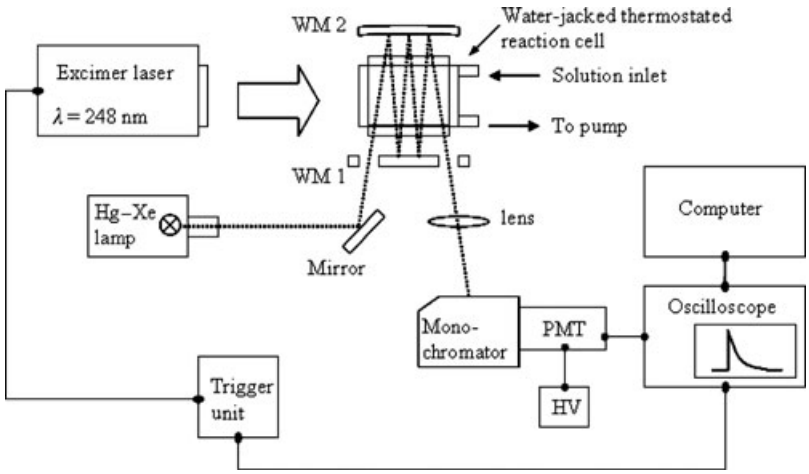

Figure 1 Laser flash photolysis setup for the study of OH radical kinetics with halogenated ethanols in aqueous solution.

To better understand the atmospheric multiphase oxidation process of HEs, in the present study the temperature dependencies of the rate constants of the reactions OH radicals with halogenated ethanols in water were investigated using laser flash photolysis and a competition kinetics method.

Correlations between reaction rates and extra kinetic parameter, such as bond dissociation energies (BDEs) or ionization potentials (IPs), have been used successfully in the literature to better understand the mechanism of a chemical reaction and to estimate unknown reaction parameters, both in the gas phase [17] and in the solution phase [20–26]. In the present study, correlations of the observed rate constants and activation energies with calculated BDEs as well as IPs are presented for the reactions of OH radicals with HEs, and finally the atmospheric implications of the study are discussed. As a part of the study, the C—H and O—H bond dissociation energies at 298.15 K and the ionization potentials of the ChAs are theoretically calculated using density functional theory (DFT). Additional calculations were performed for their fluorinated equivalents to assess the accuracy of the reported values by comparison with known experimental and previous theoretical values, and furthermore examine the trends in the calculated properties as a function of the molecular structure.

EXPERIMENTAL

Kinetic Investigations

The reactions OH radical with 2-fluoroethanol (>90%), 2,2-difluoroethanol (95%), 2,2,2-trifluoroethanol (99%) (Fluorochem Ltd., Glossop, UK), 2-chloroethanol (99%), 2,2-dichloroethanol (99%), and 2,2,2-trichloroethanol (99%) (Sigma-Aldrich, Seelze, Germany) were studied in the aqueous phase by means of laser flash photolysis combined with a competition kinetics method using the thiocyanate ion (SCN^-) as a reference system between 278 and 328 K (temperature uncertainty = ±0.1 K) and at pH = 5.5–6.5.

All chemicals were purchased at the highest purity available and used without further treatment. All solutions were freshly prepared using a Milli-Q-water system (Milipore, MI) as water source. The pH value was adjusted, if necessary, with NaOH or $HClO_4$ (Fluka, Munich, Germany).

The reaction cell is a flow-through quartz vessel (4.7-cm i.d., 7 cm long) that is thermostated by a water jacket. An excimer laser (Lambda LPX 100) has been used to generate OH radicals through the photolysis of an aqueous solution of hydrogen peroxide (5×10^{-5} M) at $\lambda = 248$ nm (excimer laser gas medium: KrF). The laser delivers an average energy of 150 mJ pro pulse that corresponds to an average OH radical concentration of 1×10^{-7} M in the cell with $[H_2O_2]_0 = 1 \times 10^{-4}$ M.

The analytical light beam generated by a high pressure Hg–Xe lamp (Hamamatsu E7536) is folded through a reaction cell 12 times with a total length of 84 cm, and it is fed to the detector, a monochromator–photomultiplier combination (Zeiss PMQ 2/Hamamatsu PMT 1P 28) connected to an oscilloscope (Gould 4050) and a computer. Further details regarding the experimental setup can be found elsewhere [24,25] and are shown in Fig. 1.

Kinetic Competition Reference System. The procedures for the kinetic measurements as well as the data analysis have been described in detail previously [24].

Briefly, OH is converted to $(SCN)_2^-$

$$OH + SCN \rightleftarrows SCNOH^- \quad (a)$$

$$SCNOH^- \rightleftarrows SCN + OH^- \quad (b)$$

$$SCN + SCN^- \rightleftarrows (SCN)_2^- \quad (c)$$

$$OH + Reactant \rightarrow Products \quad (d)$$

The second-order rate constants (k_d (M^{-1} s^{-1})) are be obtained from the following expression:

$$\frac{A_0}{A} = 1 + \frac{k_d}{k_a}\frac{[Reactant]}{[SCN^-]} \quad (1)$$

where A_0 is the light intensity absorbed by $(SCN)_2^-$ and A is the variation of the intensity when the reactant is added to the reaction solution. As the reference rate constant (k_a (M^{-1} s^{-1})), the temperature-dependent rate constant reported by Chin and Wine [27] has been used.

Five different reactant concentrations between 5×10^{-5} M and 8×10^{-3} M have been considered for the linear regression analysis. For every single reactant concentrations, the absorption signals of eight measurements were averaged. The errors given in the present study represent statistical errors for a confidence interval of 95% using the t-Student distribution.

Computational Details

All calculations were carried out with the Gaussian 98 programs suite [28], by using three DFT functionals in combination with a variety of basis sets. The B3P86 functional [29,30] was employed in the calculation of molecular geometries and vibrational frequencies, as well as in the calculation of C—H and O—H bond strengths [31,32]. Ionization potentials were calculated by the B3LYP and B3PW91 functionals [29,33], which have been shown to be sufficiently reliable for the calculation of molecular ionic properties [34,35]. Several kinds of basis sets were used (namely, variants of the 6-311G basis set, denoted as 6-311++G(2d,p) and 6-311++G(3df,2p) [36–38] as well as correlation-consistent basis sets, denoted as AUG-cc-pVDZ, cc-pVTZ, and AUG-cc-pVTZ [39–41]) to examine the effects of the basis set size and the presence of diffuse functions on the computational accuracy, and furthermore to assure the convergence of the calculated properties to a narrow range of values.

The geometry optimizations and vibrational frequencies calculations were carried out at the B3P86/AUG-cc-pVDZ level of theory for all species. Several local minima (conformers) possessing no imaginary vibrational frequencies were found for each species, and the one with the lowest energy was selected for the subsequent refinement by single-point energy calculations at higher levels of theory. All vibrational frequencies were scaled down by 0.9723 to compensate their overestimation by the B3P86/AUG-cc-pVDZ level of theory [32].

The zero-point and the thermal energies at 298.15 K were derived by considering the harmonic oscillator and the rigid-rotor approximations. They were subsequently added to the absolute electronic energies, to yield the absolute enthalpies for each species, and finally, the C—H and O—H bond dissociation energies. The vertical ionization potentials of alcohols were calculated as the difference between the absolute energies of the parent molecule and its singly ionized radical cation.

RESULTS AND DISCUSSION

Kinetic Investigations

In the literature, it is generally accepted that the reactions of hydroxyl radicals with aliphatic compounds proceed through the abstraction of the most loosely bound hydrogen atom in the molecule with the formation of the corresponding alkyl radical. In the presence of oxygen, the alkyl radical is then converted rapidly to a peroxyl radical. The aqueous-phase chemistry of the peroxyl radicals is very complex and has been reviewed elsewhere [42].

As known from previous studies as well as calculated in the present work [2,16,17], the hydrogen atoms with the weakest bond in HEs are localized in the $-CH_2$ group carrying the hydroxyl function.

Reactions of OH with Fluorinated Alcohols. The second-order rate constants obtained at five different temperatures for the following reactions ((R1)–(R3)) are summarized in Table I, whereas Fig. 2 shows the corresponding Arrhenius plots:

$$OH + CFH_2CH_2OH \rightarrow CFH_2CHOH + H_2O \quad (R1)$$

$$OH + CF_2HCH_2OH \rightarrow CF_2HCHOH + H_2O \quad (R2)$$

$$OH + CF_3CH_2OH \rightarrow CF_3CHOH + H_2O \quad (R3)$$

A clear decrease in the rate constants is observed with the increasing number of halogen atoms in the molecule. The difference in the bond dissociation energy between the nonsubstituted parent organic compounds, namely ethanol and halogen-substituted ethanols (Table II) is reflected also in the difference

Table I Rate Constants Determined in the Present Study for the Reactions of OH with 2-Fluoroethanol (k_1), 2,2-Difluoroethanol (k_2), 2,2,2-Trifluoroethanol (k_3), 2-Chloroethanol (k_4), 2,2-Dichloroethanol (k_5), and 2,2,2-Trichloroethanol (k_6)

T(K)	$k_1 \times 10^8$ (M^{-1} s^{-1})	$k_2 \times 10^8$ (M^{-1} s^{-1})	$k_3 \times 10^7$ (M^{-1} s^{-1})	$k_4 \times 10^8$ (M^{-1} s^{-1})	$k_5 \times 10^8$ (M^{-1} s^{-1})	$k_6 \times 10^8$ (M^{-1} s^{-1})
288	5.3 ± 0.7	2.1 ± 0.5	5.4 ± 0.9	7.1 ± 0.5	3.6 ± 0.7	2.2 ± 0.3
298	5.4 ± 1.8	2.8 ± 0.7	8.5 ± 2.5	8.6 ± 0.7	3.9 ± 0.8	2.4 ± 1.1
308	6.3 ± 1.1	2.9 ± 0.8	10 ± 4.0	9.6 ± 1.5	4.6 ± 1.0	2.8 ± 0.5
318	9.2 ± 5.3	3.0 ± 1.2	13 ± 8.0	10.8 ± 2.1	5.6 ± 0.6	3.5 ± 0.9
328	12.0 ± 1.0	3.2 ± 1.7	15 ± 5.1	11.1 ± 1.1	5.6 ± 0.7	3.5 ± 1.5

observed in the rate constants (Table III). A value of $k_{2nd} = 2.1 \times 10^9$ M^{-1} s^{-1} was reported for the reaction of OH with ethanol in aqueous solution [24].

Consistently, a difference in the BDE of about 10 kJ mol^{-1} corresponds to a decrease of 1 order of magnitude of the rate constant for the reaction of OH with 2-fluoroethanol and 20 kJ mol^{-1} in BDE corresponds to a decrease by 2 orders of magnitude for 2,2,2-trifluoroethanol. The large difference between the k_1 and k_2 appears to be not consistent with the calculated difference in the BDE (cf. Table IV). Halogen substitution in that case does not significantly change the calculated C—H bond strength in the $-CH_2-$ group. Therefore, the reason for the observed differences between k_1 and k_2 remains speculative. Also the obtained activation parameters show some relevant differences in the values of entropy of activation as can be seen in Table II. The entropy of activation for the reaction of OH with 2,2-difluoroethanol does not follow the trend observed in the case of ChAs, and it is significantly higher with respect to the other two FAs. Furthermore, it represents the larger negative value measured for reaction of OH with halogen-substituted organic compounds in the aqueous phase.

As most of the data presented in this work represent first measurements, a comparison with the literature is difficult. Walling et al. [20] determined first the rate constant for the reaction of OH with 2,2,2-trifluoroethanol using a steady-state method based on a Fenton reaction at room temperature. The value reported of $k_{2nd} = 2.3 \times 10^8$ M^{-1} s^{-1} is in rather large disagreement, according to the cited authors the reaction proceeds about 3 times faster than determined here. An explanation for this difference has been already indicated by Yurkova et al. [43]. As discussed in their work, in the presence of the Fenton's reagent Fe^{2+}–H_2O_2 it is not clear whether the oxidation reaction is initiated by a free hydroxyl radical or rather a reactive complex iron intermediate, for example, ferryl ion, FeO^{2+}. Depending on the nature of the organic

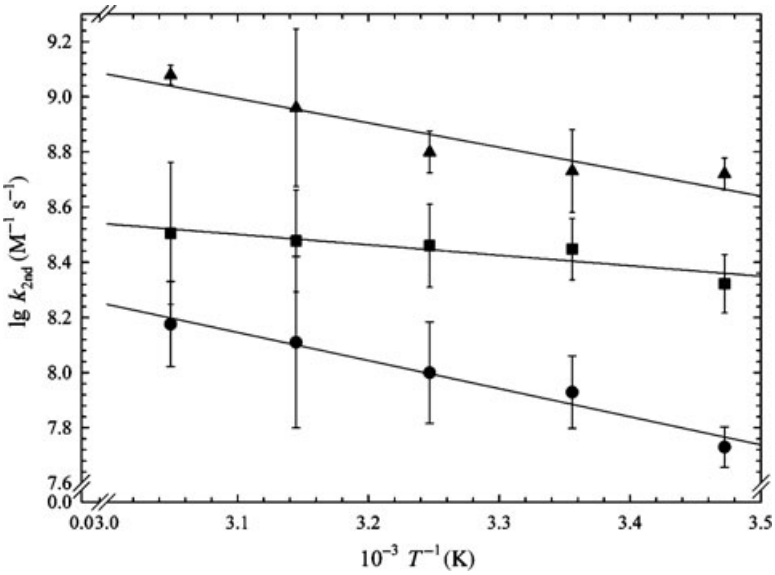

Figure 2 Arrhenius plot for the reaction of OH with 2-fluoroethanol (▲), 2,2-difluoroethanol (■), and 2,2,2-trifluoroethanol (●).

Table II Activation Parameters for H Abstraction Reactions by the OH Radical from Alcohols in Aqueous Solution

Compound	E_A (kJ mol^{-1})	A (M^{-1} s^{-1})	$\Delta S^{\ddagger}$ (J K^{-1} mol^{-1})	$\Delta H^{\ddagger}$ (kJ mol^{-1})	$\Delta G^{\ddagger}$ (kJ mol^{-1})	Reference	BDE (C—H) (kJ mol^{-1})	Reference
2-Fluoroethanol	17 ± 10	$(5.7 \pm 0.8) \times 10^{11}$	$-(28 \pm 4)$	14.5 ± 9	23 ± 17	This work	399.6	This work
2,2-Difluoroethanol	7 ± 7	$(4.5 \pm 0.5) \times 10^{9}$	$-(69 \pm 8)$	4.6 ± 4	25 ± 26	This work	399.5	This work
2,2,2-Trifluoroethanol	20 ± 7	$(2.0 \pm 0.1) \times 10^{11}$	$-(37 \pm 4)$	17 ± 6	28 ± 12	This work	409.0	This work
2-Chloroethanol	9 ± 4	$(3.0 \pm 0.2) \times 10^{10}$	$-(53 \pm 3)$	6 ± 3	22 ± 10	This work	394.1	This work
2,2-Dichloroethanol	10 ± 4	$(2.1 \pm 0.2) \times 10^{10}$	$-(55 \pm 5)$	7 ± 3	24 ± 12	This work	399.4	This work
2,2,2-Trichloroethanol	10 ± 5	$(1.6 \pm 0.1) \times 10^{10}$	$-(58 \pm 4)$	8 ± 4	25 ± 13	This work	404.0	This work
Ethanol	10 ± 5	$(1.0 \pm 0.1) \times 10^{11}$	$-(42 \pm 4)$	8 ± 4	20 ± 12	[24]	389	[24]
1-Propanol	8 ± 6	$(5.6 \pm 0.6) \times 10^{10}$	$-(47 \pm 5)$	6 ± 4	20 ± 17	[24]	385	[24]
2-Propanol	8 ± 2	$(6.3 \pm 0.3) \times 10^{10}$	$-(47 \pm 2)$	6 ± 2	20 ± 6	[22]	381	[22]
1-Butanol	8 ± 1	$(1.0 \pm 0.1) \times 10^{11}$	$-(42 \pm 1)$	5 ± 1	18 ± 2	[22]	385	[22]

reactants, the latter reaction might significantly contribute to the overall rate constant leading to an overestimation of the observed rate constant. The reactivity of the Fe(IV) species FeO^{2+} is described in the literature [44,45].

Reactions of OH with Chlorinated Alcohols. In the same range of temperature applied for the fluorinated ethanols, the kinetics of the following reactions with chlorinated alcohols has been studied:

$$OH + CH_2ClCH_2OH \rightarrow CH_2ClCHOH + H_2O \quad (R4)$$

$$OH + CHCl_2CH_2OH \rightarrow CHCl_2CHOH + H_2O \quad (R5)$$

$$OH + CCl_3CH_2OH \rightarrow CCl_3CHOH + H_2O \quad (R6)$$

The second-order rate constants for the reactions of OH radicals with the series of chlorinated alcohols obtained as a function of the temperature are summarized in Table I. To the best of the authors' knowledge, these values are the first temperature-dependent measurements for reactions (R4)–(R6) in aqueous solution. The Arrhenius plots are presented in Fig. 3, and the derived activation parameters are summarized in Table II together with the bond dissociation energies of the weakest C—H bond in the respective molecules. The activation parameters have been calculated as previously described in [24].

In the case of 2-chloroethanol, the comparison with a previous study performed at room temperature shows relatively good agreement. In that study, Anbar and Neta [21] determined the second-order rate constant as $k_4 = 9.6 \times 10^8$ M^{-1} s^{-1} using γ-radiolysis to generate

Table III Aqueous and Gas-Phase Rate Constants of the Reactions OH Radicals with Small Linear Alcohols

No.	Compound	k (298 K) Aqueous phase (M^{-1}s^{-1})	Reference	k (298 K) Gas phase (M^{-1}s^{-1})	Reference
1	2-Fluoroethanol	5.4×10^8	This work	8.5×10^8	[2]
				1.0×10^9	[19]
2	2,2-Difluoroethanol	2.8×10^8	This work	2.7×10^8	[2]
3	2,2,2-Trifluoroethanol	0.8×10^8	This work	0.74×10^8	[2]
		1.8×10^8	[57]	0.6×10^8	[16]
		2.3×10^8	[20]	0.57×10^8	[57]
				0.57×10^8	[58]
4	2-Chloroethanol	8.6×10^8	This work	7.7×10^8	[57]
		9.6×10^8	[57]		
5	2,2-Dichloroethanol	3.9×10^8	This work	–	–
6	2,2,2-Trichloroethanol	2.4×10^8	This work	1.5×10^8	[57]
		3.2×10^8	[57]		
		4.2×10^8	[20]		
7	Ethanol	2.1×10^9	[24]	1.9×10^9	[47][a]
8	1-Propanol	3.2×10^9	[24]	3.3×10^9	[47][a]
9	1-Butanol	4.1×10^9	[22]	5.1×10^9	[47][a]

[a] Data reported represent the average of existing literature values [47].

Table IV Experimental and Calculated C—H and O—H Bond Dissociation Energies (in kJ mol^{-1}) for Ethanol, Fluorinated, and Chlorinated Ethanols

Bond	Experimental[a]	Calculated (This Study)	Calculated [31][b]
CH_2CH_2OH—H	419.7 ± 8.4	430.0	424.4
CH_3CHOH—H		396.0	391.0
CH_3CH_2O—H	436.0 ± 4.2	433.7	438.3
$CHFCH_2OH$—H		425.0	415.2
CH_2FCHOH—H		399.6	392.5
CH_2FCH_2O—H		463.9	450.5
CF_2CH_2OH—H		428.7	418.1
CHF_2CHOH—H		399.5	390.7
CHF_2CH_2O—H		452.5	456.9
CF_3CHOH—H		409.0	397.8
CF_3CH_2O—H		462.3	467.2
$CHClCH_2OH$—H		420.9	
$CH_2ClCHOH$—H		394.1	
CH_2ClCH_2O—H		447.4	
CCl_2CH_2OH—H		412.8	
$CHCl_2CHOH$—H		399.4	
$CHCl_2CH_2O$—H		456.3	
CCl_3CHOH—H		404.0	
CCl_3CH_2O—H		458.7	

The calculated BDEs are represented as the average of the three most accurate theoretical values obtained at the B3P86/AUG-cc-pVTZ, B3P86/AUG-cc-pVDZ, and B3P86/6-311++G(2df,p) levels of theory.

[a] From enthalpies of formation in [47,48].

[b] Bond dissociation energies calculated at the B3P86/6–311++G(3df,2p) level of theory, using molecular structures optimized at the B3P86/6–31G(d) level, without taking into account of empirical corrections to the radical species energies.

the radicals and applied competition kinetics using the reaction with ethanol as reference. The kinetic results are collected in Table III.

In contrast, Walling et al. [20] obtained a value ($k_6 = 4.2 \times 10^8\ M^{-1}\ s^{-1}$) for the second-order rate constant for the reaction of OH with 2,2,2-trichloroethanol that is two times larger than the value presented here. Also, in this case the difference in the measured rate constants might be explained as discussed for the reaction of OH with 2,2,2-trifluoroethanol.

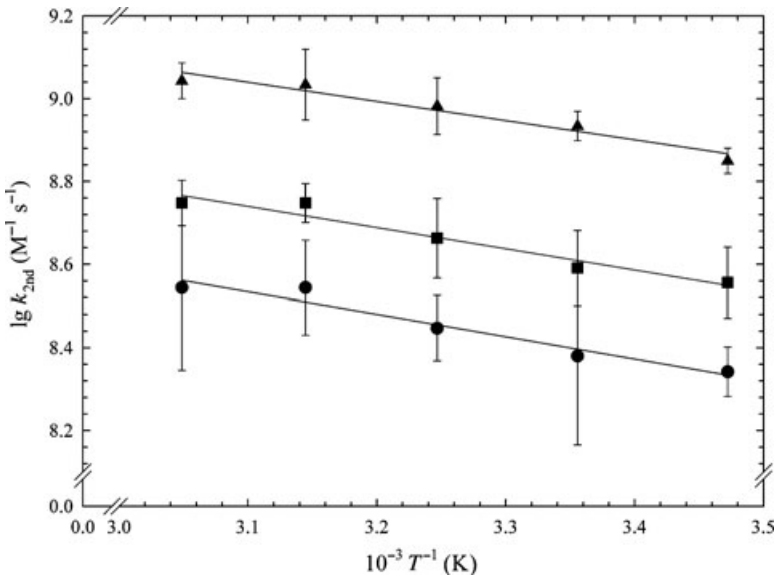

Figure 3 Arrhenius plot for the reaction of OH with 2-chloroethanol (▲), 2,2-dichloroethanol (■), and 2,2,2-trichloroethanol (●).

Reactivity Comparison. The analysis of the activation parameters (Table II) shows similar values for all the compounds. A more detailed description of how the activation parameters have been derived can be found elsewhere [24,46]. The rate constants for the reactions of OH with ChAs appear to have the same dependence on temperature as observed for the reaction of OH with ethanol and other simple aliphatic alcohols with an average value of 10 kJ $mol^{-1}$for the energy of activation. A different trend is observed in the case of fluorine-substituted alcohols. Whereas 2,2-fluoroethanol shows an activation energy close to the chlorine-substituted alcohols, 2-fluoroethanol and 2,2,2-trifluoroethanol have significant higher activation energies.

When nonsubstituted alcohols and ChAs are considered, the entropies of activation indicate that similar transition state structures can be expected within the same groups of compounds. This does not apply in the case of FAs, where a trend in the results is difficult to identify.

Theoretical Calculations

The most stable conformers of CH_2ClCH_2OH, $CHCl_2CH_2OH$, and CCl_3CH_2OH, as well as of their singly dehydrogenated radicals $CH_{3-n}Cl_nCHOH$ ($n = 1, 2, 3$), calculated at the B3P86/AUG-cc-pVDZ level of theory, have been identified and their bond lengths, bond angles, and the dihedral angles between the O—C—C/C—C—X (X = Cl or H) and H—O—C/O—C—C planes are summarized and shown in Fig. 4.

The absolute electronic energies for all species were found to depend on the arrangement of the OH group, as in fluorinated ethanols [31]. For CH_3CH_2OH and CH_3CHOH, there is a slight increase in the energy by ca. 1 kJ mol^{-1} when the OH group is arranged toward the CH_3 group due to the unfavorable steric repulsions. On the other hand, for all ChAs and their OH groups, there is a stabilization when the OH group is facing Cl atoms, due to the attractive intramolecular C—Cl···H—O interactions. The energy barrier of the OH internal rotation depends on the degree of substitution by chlorine atoms, reaching a maximum of ca. 13 kJ mol^{-1} for CCl_3CH_2OH.

The C—H and O—H bond dissociation energies of ethanol as well as fluorinated and chlorinated ethanols were calculated at five levels of theory, all consisting of the B3P86 functional in combination with the basis sets AUG-cc-pVDZ, cc-pVTZ, AUG-cc-pVTZ, 6-311++G(2df,p), and 6-311++G(3df,2p), by taking into account empirical corrections of the electronic energies of the radical species [32] to lower the deviation from the experimental values inferred from the corresponding standard enthalpies of formation [47,48]. The variation of all BDEs at these levels of theory was small and never exceeded 4 kJ mol^{-1}, indicating that the calculated values have converged sufficiently to a narrow range of accurate values. However, a negligible dependence on the size of the basis set was noted, and the accuracy of the calculated BDEs was slightly improved by the presence of diffuse functions. The average values of the empirically corrected results at the three most accurate levels of theory (B3P86/AUG-cc-pVTZ, B3P86/AUG-cc-pVDZ, and B3P86/6-311++G(2df,p)) are shown in Table IV.

The largest deviation from experimental values is ca. 10 kJ mol^{-1} for the H—CH_2CH_2OH bond, and all remaining deviations are lower than 6 kJ mol^{-1}.

The ionization potentials of ethanol as well as FAs and ChAs were calculated at 10 levels of theory, consisting of the B3LYP and B3PW91 functionals and the five basis sets discussed above. The mean deviation from experimental values [49] was rather insensitive to the level of theory, on the order of 0.12–0.20 eV. The smallest deviations were presented by the B3PW91 functional, and the agreement with experimental values was slightly deteriorating by the presence of diffuse functions in the basis sets. The average value of the ionization potentials of the three most accurate levels of theory (B3PW91/cc-pVTZ, B3PW91/6-311++G(3df,2p), and B3LYP/cc-pVTZ) is shown in Table V.

The average deviation of the calculated IPs from experimental values is quite low, in the order of 0.03 eV. However, the comparison with the literature data remains incomplete due to the lack of data for CHF_2CH_2OH and $CHCl_2CH_2OH$.

Table V Experimental and Calculated Vertical Ionization Potentials (in eV) for Ethanol, Fluorinated, and Chlorinated Ethanols

Molecule	Experimental [49]	Calculated (This Study)
CH_3CH_2OH	10.47	10.54
CH_2FCH_2OH	10.66	10.81
CHF_2CH_2OH		11.12
CF_3CH_2OH	11.49	11.63
CH_2ClCH_2OH	10.66	10.55
$CHCl_2CH_2OH$		10.64
CCl_3CH_2OH	10.94	10.86

The calculated IPs are represented as the average of the three most accurate theoretical values obtained at the B3PW91/cc-pVTZ, B3LYP/cc-pVTZ, and B3PW91/6-311++G(3df,2p) levels of theory.

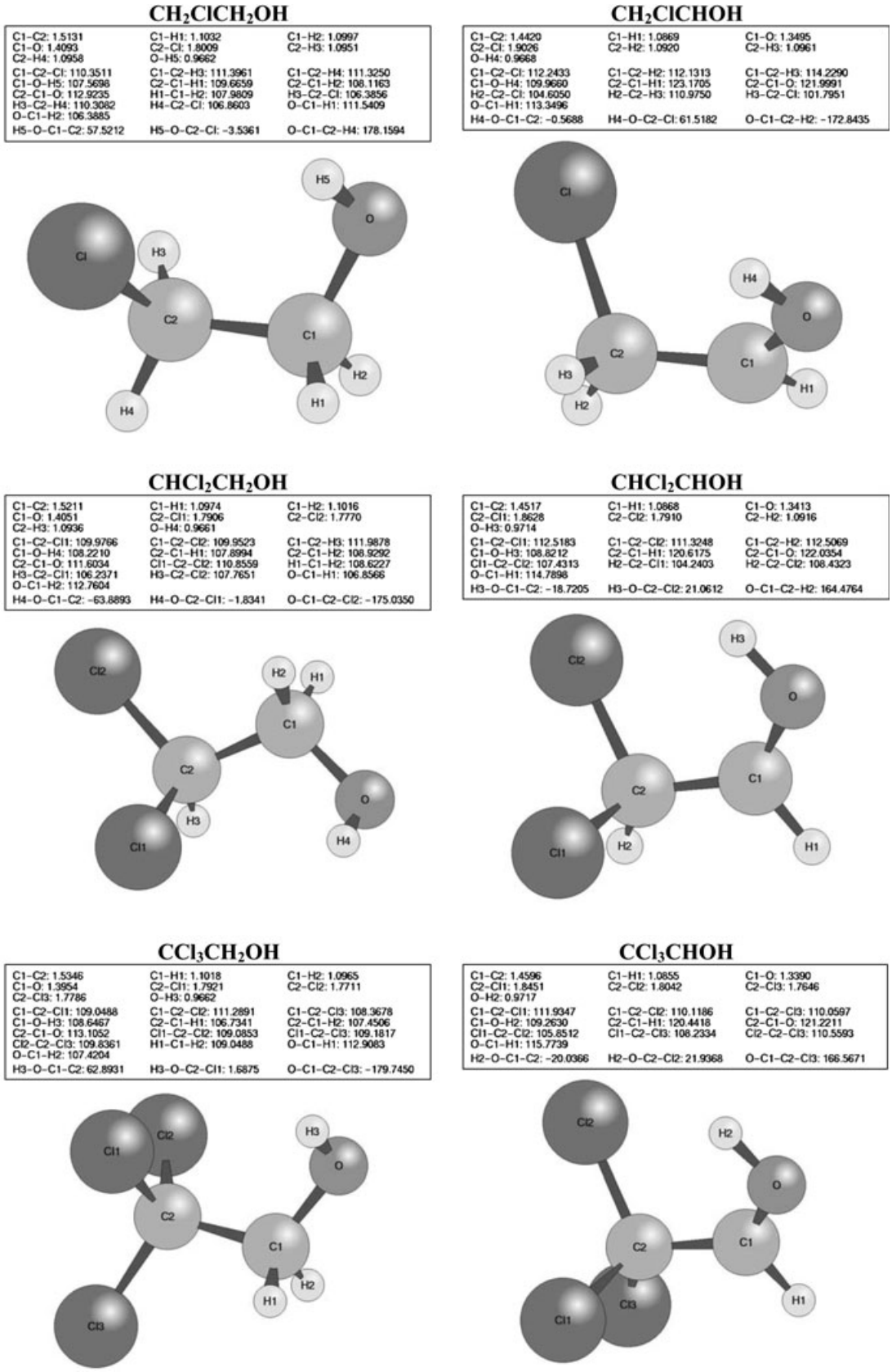

Figure 4 Optimized structures for the parent $CH_{(3-n)}Cl_nCH_2OH$ ethanols and $CH_{(3-n)}Cl_nCHOH$ radicals ($n = 1,2,3$) at the B3P86/AUG-cc-pVDZ level of theory. Bond lengths, bond angles, and important dihedral angles are also shown.

Reactivity Correlations

Evans and Polanyi studied the existing relationships between the thermochemistry of a reaction and the activation barrier represented by the activation energy E_A, which for a given reaction is related to the heat of reaction, ΔH_R, by the following equation [50]:

$$E_A = a + b\Delta H_R \tag{2}$$

where a and b represent empirical constants.

For a series of reactions that proceed through the same reaction mechanism, it follows that a correlation between the reaction enthalpy and the bond dissociation energy BDE (C—H) of the weakest bond broken during the reaction should exist:

$$\Delta H_R \sim \text{BDE(C—H)} \tag{3}$$

As shown elsewhere [22–25], a correlation can be then written

$$\log k = \log A - \frac{E_A}{RT} = \left(\log A - \frac{a'}{RT}\right) - \frac{b'}{RT} \cdot \text{BDE(C—H)} \tag{4}$$

The Evans–Polanyi plot in the form of energy of activation (E_A) against the bond dissociation energies of the weakest bond for the investigated reactions of OH with small aliphatic alcohols in aqueous solution is presented in Fig. 5. Here, the bond strengths for the C—H bonds in the halogenated compounds that have been calculated in the present work (cf. Table IV) have directly been used.

From the regression line of the Evans–Polanyi plot, the following correlation can be obtained:

$$E_A/\text{kJ mol}^{-1} = -(110 \pm 107) + (0.3 \pm 0.28) \cdot \text{BDE(C—H)/kJ mol}^{-1} \tag{5}$$

with $n = 10$ and $r = 0.65$.

In Eq. (5), only the halogenated ethanols together with four not substituted aliphatic alcohols are considered. The obtained correlation results are different with respect to the available literature correlations (Eq. (6) [22] and Eq. (7) [25]) for aqueous-phase reactions of OH radicals with oxygenated organic compounds. Thus, the authors recommend to restrict the use of Eq. (5) only for the estimation of kinetic data for reactions of halogen-substituted alcohol with OH in aqueous solution.

$$E_A/\text{kJ mol}^{-1} = -(52 \pm 33) + (0.16 \pm 0.08) \cdot \text{BDE(C—H)/kJ mol}^{-1} \quad (n = 16; r = 0.75) \tag{6}$$

$$E_A/\text{kJ mol}^{-1} = -(52 \pm 34) + (0.16 \pm 0.09) \cdot \text{BDE(C—H)/kJ mol}^{-1} \quad (n = 17; r = 0.69) \tag{7}$$

Furthermore, as can be seen from the plot and Table II, the values of the energy of activation for 2-fluoroethanol and 2,2,2-trifluoroethanol stay far from the set of data as well as from the average value observed for the reactions of OH radical with organic compounds in the aqueous phase.

It has also been demonstrated [22–25] that equivalent H atoms in the molecule will contribute to the same extent to the observed rate constant. Thus, Eq. (4) can also be rewritten as

$$\log\left(\frac{k}{n_H}\right) = \log k_H = \left(\log A - \frac{a'}{RT}\right) - \frac{b'}{RT} \cdot \text{BDE(C—H)} \tag{8}$$

Using the data reported in Table VI, the corresponding plot is shown in Fig. 6.

In this case, the following correlation is obtained (Eq. (9)):

$$\log\left(k_H/\text{M}^{-1}\text{s}^{-1}\right) = (33 \pm 3) - (0.06 \pm 0.008)\ \text{BDE/kJmol}^{-1} \tag{9}$$

with $n = 11$ and $r = 0.98$.

Gligorovski and Herrmann [25] presented a correlation where an extended data set is considered for reactions of OH radicals with organic carbonyl compounds in the aqueous phase, using BDE values calculated with the incremental method of Benson [51]. The reasonably good agreement between (Eq. (9)) and the previous expression [25] allows the use of this empirical relation also for the prediction of reactivity for a wider selection of compounds including carbonyl compounds and alcohols.

Equations (5) and (9) permit the estimation of OH rate constants for H-abstraction reactions from halogen-substituted alcohols in aqueous solution at $T = 298$ K when measurements are not available. Furthermore, the user must be aware of the uncertainty of the obtained results due to the experimental and BDE estimation errors.

Furthermore, the kinetic parameters for hydrogen abstraction reactions may be also empirically correlated either with the number and nature of constituent atom groups via additivity rules or with molecular property values, such as ionization potentials [52,53], leading to various structure–activity relationships. As shown previously for OH radical gas-phase reactions with halogenated ethanols [2], a correlation

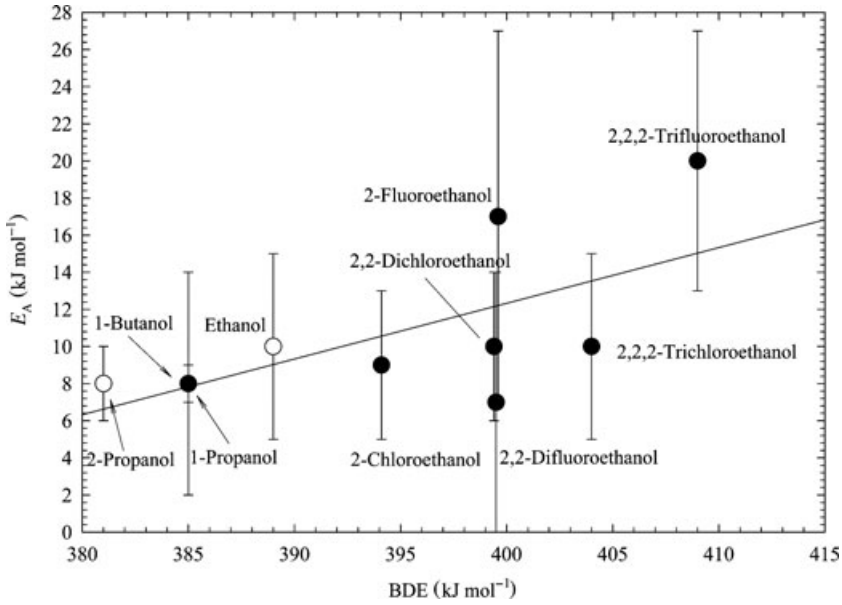

Figure 5 Evans–Polanyi plot in the form of energy of activation (E_A/kJ mol^{-1}) vs. bond dissociation energy (BDE/kJ mol^{-1}). This work (●). Literature values (○).

does exist between the sum of the Pauling's electronegativities (SPE) [48] and the logarithm of the measured rate constants.

As shown in Fig. 7, a correlation (Eq. (10)) has been obtained plotting the logarithm of the observed rate constants as a function of the electronegativity of the CX_3 group.

$$\log(k_{298}/M^{-1}s^{-1}) = (11.4 \pm 0.9) - (0.27 \pm 0.08) \cdot \text{SPE} \quad (10)$$

where $n = 7$ and $r = 0.96$. The values of electronegativities used to calculate the SPE are F (4), Cl (3), H (2.1), and for C (2.5) [48].

The linearity of the plot suggests that the measured rate constants correlate well with the empirically derived electronegativity of the terminal methyl group. It also reflects the decrease of the reactivity of halogenated ethanols toward the electrophilic OH due to the electron-withdrawing effects of the halogen substituents. In addition, this linear relationship can be used to determine the rate constants of those OH reactions with HEs that have not been determined experimentally.

A good correlation can be also obtained comparing the aqueous- and gas-phase rate constants (Table III) for the reactions of OH radicals with small HEs. The linear relationship is shown in Fig. 8, and the following

Table VI Rate Constants (298 K) and for Equivalent Abstractable Hydrogen Atom (k_H) for Reactions of the OH Radical in Aqueous Solution

Compound	k (298 K) (M^{-1} s^{-1})	n_H	k_H (M^{-1} s^{-1})	log k_H	Reference
2-Fluoroethanol	5.4×10^8	2	2.7×10^8	8.4	This work
2,2-Difluoroethanol	2.8×10^8	2	1.4×10^8	8.1	This work
2,2,2-Trifluoroethanol	0.8×10^8	2	0.4×10^8	7.6	This work
2-Chloroethanol	8.6×10^8	2	4.3×10^8	8.6	This work
2,2-Dichloroethanol	3.9×10^8	2	2.0×10^8	8.3	This work
2,2,2-Trichloroethanol	2.4×10^8	2	1.2×10^8	8.1	This work
Ethanol	2.1×10^9	2	1.1×10^9	9.0	[24]
1-Propanol	3.2×10^9	2	1.6×10^9	9.2	[24]
2-Propanol	2.1×10^9	1	2.1×10^9	9.3	[22]
1-Butanol	4.1×10^9	2	2.1×10^9	9.3	[22]
tert-Butanol	5.0×10^8	9	0.6×10^8	7.7	[22]

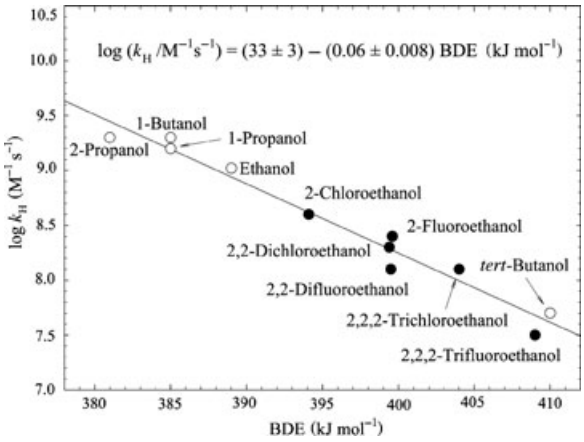

Figure 6 Evans–Polanyi plot in the form of log k_H ($M^{-1}s^{-1}$) vs. BDE (kJ mol^{-1}). This work (●). Literature values (○).

equation can be written:

$$k_{298,\text{aqueous}}/\text{M}^{-1}\text{s}^{-1} = (0.11 \pm 0.26) \times 10^9 + (0.84 \pm 0.12) k_{298,\text{gas}}/\text{M}^{-1}\text{s}^{-1} \qquad (11)$$

where $n = 8$ and $r = 0.99$.

The fact that the slope of Eq. (11) is close to 1 indicates that the rate constants of aqueous-phase reactions of halogenated alcohols with OH radicals are similar to the gas-phase reactions. However, for a detailed comparison between aqueous- and gas-phase processes phase-transfer parameters (e.g., Henry's constant values) as well as radical concentrations must be considered. A more detailed discussion on this issue is given in the next section. Equation (11) can be used alternatively to estimate the rate constant of OH reactions with HEs when the rate constant is known for one of the two phases.

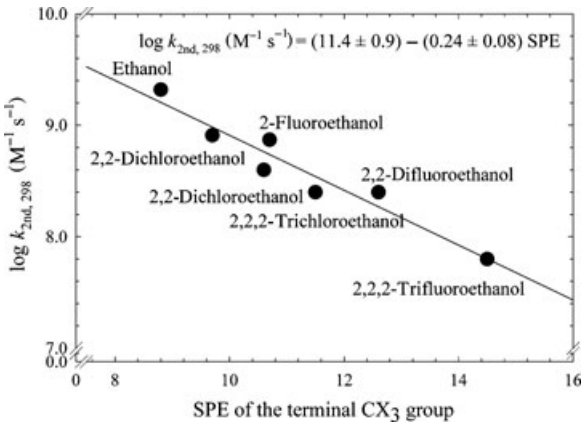

Figure 7 Plot of the logarithm of the second-order rate constants (log k/M^{-1} s^{-1}) vs. the sum of Pauling electronegativities of the terminal CX_3 (X = H-, Cl-, F-) group.

ATMOSPHERIC IMPLICATIONS

The atmospheric degradation of HEs is initiated by radical reactions in the gas phase by OH and, possibly, NO_3 radicals, or halogen atoms. Sellevåg et al. [2] calculated the tropospheric lifetime of fluorinated ethanols to be between 20 and 117 days considering their gas-phase reactions with OH as the major sink. The primary oxidation products, fluorinated aldehydes, are suggested to be not harmful to the environment due to their small atmospheric concentration in the sub-ppb range. Secondary gas-phase products such as CHFO and CF_2O will be incorporated into droplet/aerosols and hydrolyzed to give CO, CO_2, and HF within days. A photolytic decomposition might also occur; however, Vasiliev et al. [54] ruled out this possible degradation channel in the case of 2,2,2-trifluoroethanol.

The removal from the atmosphere through wet deposition has been also suggested [3], and it has been estimated to account up to 30% for 2,2,2-trifluoroethanol using a simple model, where the authors used a rather high value as global average for liquid water content (LWC) that might lead to an overestimation of the uptake in cloud water. It must also be mentioned that no liquid phase sinks are included though the atmospheric lifetime of these compounds depends on OH concentrations and their reactivity in the different phases.

As reported above, FAs are relatively soluble in water and they may be removed from the troposphere by uptake in cloud droplets and further oxidized in water droplets before the removal through wet deposition processes. In-cloud processes should be taken in account since CF_3-containing FAs may lead to trifluoroacetic acid (TFA) formation. With the possible exception of TFA, the hydrolysis products are ubiquitous, naturally occurring species that have little adverse environmental impact.

For the evaluation of the tropospheric lifetimes of substituted alcohols in the gas and aqueous phases, lifetimes have been calculated using the measured kinetic constants and available modeled OH radical concentrations. The radical concentrations substantially depend on the atmospheric environmental conditions. Therefore, modeled maximum and minimum gas- and aqueous-phase concentrations of OH radicals for different atmospheric regimes (Table VII) have been used for the estimation of the tropospheric lifetimes in both phases. The radical concentrations were derived from SPACCIM model [55] simulations using a complex multiphase chemistry mechanism

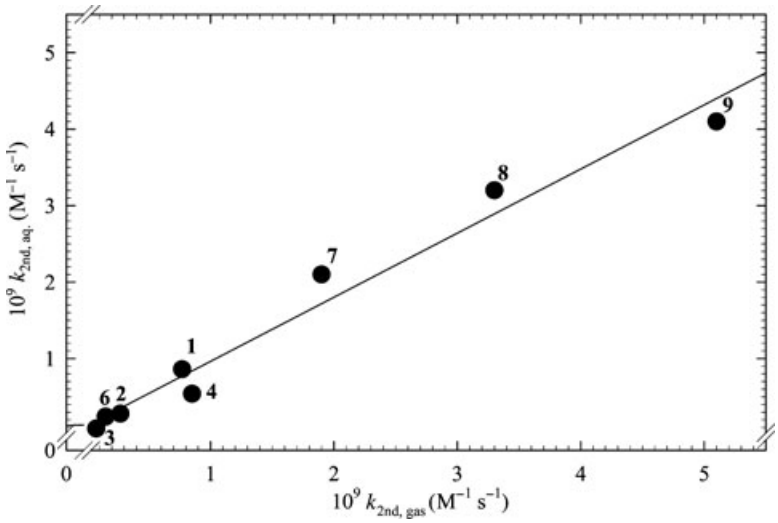

Figure 8 Plot of the measured aqueous-phase rate constants for the reaction of OH radicals with a series of linear alcohols vs. the corresponding gas-phase rate constants at 298 K. Numbering refers to Table III.

RACM-MIM2(extended)/CAPRAM3.0i [56]. Model simulations have been performed for three scenarios. These are anthropogenic polluted (urban), continental background (remote), and marine tropospheric regimes based on radiation conditions of 19 June (summer solstice, 45°N). The derived minimum and maximum OH concentrations correspond to nighttime and daytime conditions, respectively. The both aqueous-phase concentrations summarized in Table VII correspond to cloud-free conditions at 90% relative humidity level (deliquescent aerosol particles) and in-cloud conditions (cloud droplets) and represent the total concentrations as integrated of the aqueous particle/cloud droplet spectrum.

In Table VIII, the atmospheric lifetimes for the three scenarios using the concentration of OH radicals as in Table VII are then reported.

As can be seen in Table VIII, halogenated alcohols are processed faster in the aqueous phase than in the gas phase. It should be noted that the aqueous-phase lifetimes are in most of the cases 2 orders of magnitude smaller than the corresponding gas-phase lifetimes. However, the calculated lifetimes do not account for the relative distribution of the considered compounds between the gas and aqueous phase. At present, the missing Henry's constant values for the halogenated alcohols do not allow more precise conclusions of the fate of HEs, but the kinetic data obtained here suggested clearly that the aqueous-phase processes can establish important sinks for HEs in the troposphere.

SUMMARY

The kinetic investigations presented here support the view that OH radicals react with saturated organic compounds through the abstraction of the hydrogen atom with the weakest bond dissociation energy in the molecule. In the case of the halogen-substituted ethanols, the kinetic and theoretical results indicate that the H atoms abstracted are the ones bonded to the

Table VII Modeled Concentrations of OH Radical in the Gas Phase as well as Aqueous Phase (Cloud Droplet and Deliquescent Particle Conditions; See Text)

		A	B	C
Scenario		Gas Phase (molec. cm^{-3})	Cloud Droplets (mol L^{-1})	Wet Particles (mol L^{-1})
Remote scenario	Min.	1.2×10^5	1.0×10^{-14}	4.0×10^{-13}
	Max.	4.2×10^5	5.0×10^{-14}	3.6×10^{-12}
Marine scenario	Min.	1.2×10^6	5.0×10^{-14}	1.0×10^{-14}
	Max.	3.3×10^6	5.3×10^{-12}	6.0×10^{-14}
Urban scenario	Min.	1.5×10^5	5.0×10^{-16}	5.0×10^{-14}
	Max.	1.5×10^6	1.0×10^{-14}	8.0×10^{-13}

Table VIII Calculated Lifetimes of Halogenated Ethanols Based on Modeled Gas- and Aqueous-Phase OH Radical Concentrations (Table VII) for Three Different Tropospheric Pollution Conditions (Remote, Marine, Urban)

		Lifetime, Remote Conditions			Lifetime, Marine Conditions			Lifetime, Urban Conditions		
Compound		A	B	C	A	B	C	A	B	C
2-Fluoroethanol	Min.	18	0.43	0.14	2.3	0.004	8.6	5	2.1	0.64
	Max.	63	2.1	1.3	6.3	0.43	51	50	43	10
2,2-Difluoroethanol	Min.	61	0.89	0.3	7.8	0.008	18	17	4.5	1.3
	Max.	210	4.5	2.7	21	0.89	110	170	89	21
2,2,2-Trifluoroethanol	Min.	270	1.4	0.48	34	0.014	29	75	7.2	2.2
	Max.	930	7.2	4.3	93	1.4	170	750	140	35
2-Chloroethanol	Min.	21	0.26	0.09	2.7	0.002	5.2	6	1.3	0.39
	Max.	75	1.3	0.78	7.5	0.26	31	60	26	6.2
2,2-Dichloroethanol	Min.	–	0.59	0.2	–	0.006	12	–	3	0.89
	Max.	–	3	1.8	–	0.59	71	–	59	14
2,2,2-Trichloroethanol	Min.	110	0.7	0.2	14	0.007	14	31	3.5	1.1
	Max.	390	3.5	2.1	39	0.7	84	310	70	17
Ethanol	Min.	8.7	0.1	0.04	1.1	0.001	2.2	2.4	0.55	0.17
	Max.	30	0.55	0.33	3.0	0.11	13	24	11	2.6

All the lifetimes are expressed in days.
A, B, and C refer to the OH radical concentrations reported in Table VII for the corresponding scenario.

carbon atom carrying the alcoholic function. Computational methods have been applied for the estimation of bond dissociation energies and ionization potentials of halogenated ethanols.

Three different reactivity correlations have been obtained and can be applied for the estimation of unknown rate constants with focus on reactions of OH radicals with halogen-substituted alcohols in aqueous solution. The comparison between the gas- and aqueous-phase rate coefficients for the investigated compounds shows that solution processes are competitive, and they should be included in environmental assessments on halogenated ethanols.

The computational work was partially supported by the "Excellence in the Research Institutes" Program, Action 3.3.1, cofunded by the Greek Ministry of Development (GSRT) and the European Union (EU).

BIBLIOGRAPHY

1. Molina, M. J.; Molina, L. T.; Kolb, C. E. Annu Rev Phys Chem 1996, 47, 327–367.
2. Sellevåg, S. R.; Nielsen, C. J.; Søvde, O. A.; Myhre, G.; Sundet, J. K.; Stordal, F.; Isaksen, I. S. A. Atmos Environ 2004, 38/39, 6725–6735.
3. Chen, L.; Takenaka, N.; Bandow, H.; Maeda, Y. Atmos Environ 2003, 37, 4817–4822.
4. Handbook of Physical Properties of Organic Chemicals; CRC Press: Boca Raton, FL, 1997.
5. Lovejoy, E. R.; Huey, L. G.; Hanson, D. R. J Geophys Res, Atmos 1995, 100(D9), 18775–18780.
6. Hage, J. C.; Hartmans, S. Appl Environ Microbiol 1999, 65, 2466–2470.
7. Hashimoto, A.; Iwasaki, K.; Nakasugi, N.; Nakajima, M.; Yagi, O. Biosci Biotechnol Biochem 2002, 66, 385–390.
8. Hutson, D. H.; Hoadley, E. C.; Pickering, B. A. Xenobiotica 1971, 1, 593–611.
9. Gruss, M.; Hempelmann, G.; Scholz, A. Neuroreport 2002, 13, 853–856.
10. Toropov, A. A.; Duchowicz, P.; Castro, E. A. Int J Mol Sci 2003, 4, 272–283.
11. Biester, H.; Keppler, F.; Putschew, A.; Martinez-Cortizas, A.; Petri, M. Environ Sci Technol 2004, 38, 1984–1991.
12. Ballschmiter, K. Chemosphere 2003, 52, 313–324.
13. Neidleman, S. L.; Geigert, J. Biohalogenation: Principles, Basic Roles and Applications; Wiley: New York, 1986.
14. O'Hagan, D.; Harper, D. B. J Fluorine Chem 1999, 100, 127–133.
15. O'Hagan, D.; Robins, R. J.; Wilson, M.; Wong, C. W. J Chem Soc, Perkin Trans 1 1999, 15, 2117–2120.
16. Tokuhashi, K.; Nagai, H.; Takahashi, A.; Kaise, M.; Kondo, S.; Sekiya, A.; Takahashi, M.; Gotoh, Y.; Suga, A. J Phys Chem A 1999, 103, 2664–2672.
17. Kelly, T.; Manning, M.; Bonard, A.; Wenger, J.; Treacy, J.; Sidebottom, H. In Proceedings from the EUROTRAC-2 Symposium 2000; Midgley, P. M.; Reuther, M.; Williams, M. (Eds.); Springer-Verlag: Berlin, 2001.

18. Chen, L.; Fukuda, K.; Takenaka, N.; Bandow, H.; Maeda, Y. Int J Chem Kinet 2000, 32, 73–78.
19. Rajakumar, B.; Burkholder, J. B.; Portmann, R. W.; Ravishankara, A. R. Phys Chem Chem Phys 2005, 7(12), 2498–2505.
20. Walling, C.; El-Taliawi, G. M; Johnson, R. A. J Am Chem Soc 1974, 96, 133–139.
21. Anbar, M.; Neta, P. J Chem Soc A 1967, 834–837.
22. Herrmann, H. Chem Rev 2003, 103(12), 4691–4716.
23. Monod, A.; Poulain, L.; Grubert, S.; Voisin, D.; Wortham, H. Atmos Environ 2005, 39, 7667–7688.
24. Ervens, B.; Gligorovski, S.; Herrmann, H. Phys Chem Chem Phys 2003, 5(9), 1811–1824.
25. Gligorovski, S.; Herrmann, H. Phys Chem Chem Phys 2004, 6(16), 4118–4126.
26. Poole, J. S.; Shi, X. F.; Hadad, C. M.; Platz, M. S. J Phys Chem A 2005, 109(11), 2547–2551.
27. Chin, M.; Wine, P. H. A. J Photochem Photobiol A 1992, 69(1), 17–25.
28. Frisch, M. J.; Trucks, G. W.; Schlegel, H. B.; Scuseria, G. E.; Robb, M. A.; Cheeseman, J. R.; Zakrzewski, V. G.; Petersson, G. A.; Montgomery, J. A., Jr.; Stratmann, R. E.; Burant, J. C.; Dapprich, S.; Millam, J. M.; Daniels, A. D.; Kudin, K. N.; Strain, M. C.; Farkas, O.; Tomasi, J.; Barone, V.; Cossi, M.; Cammi, R.; Mennucci, B.; Pomelli, C.; Adamo, C.; Clifford, S.; Ochterski, J.; Petersson, G. A.; Ayala, P. Y.; Cui, Q.; Morokuma, K.; Malick, D. K.; Rabuck, A. D.; Raghavachari, K.; Foresman, J. B.; Cioslowski, J.; Ortiz, J. V.; Stefanov, B. B.; Liu, G.; Liashenko, A.; Piskorz, P.; Komaroni, I.; Gomperts, R.; Martin, R. L.; Fox, D. J.; Keith, T. A.; Al-Laham, M. A.; Peng, C. Y.; Nanayakkara, A.; Gonzalez, C.; Challacombe, M.; Gill, P. M. W.; Johnson, B. G.; Chen, W.; Wong, M. W.; Andreas, J. L.; Head-Gordon, M.; Replogle, E. S.; Pople, J. A. Gaussian 98, A.7; Gaussian, Inc.: Pittsburgh, PA, 1998.
29. Becke, A. D. J Chem Phys 1993, 98, 5648–5652.
30. Perdew, J. P.; Burke, K; Wang, Y. Phys Rev B 1996, 54, 16533–16539.
31. Papadimitriou, V. C.; Prosmitis, A. V.; Lazarou, Y. G.; Papagiannakopoulos, P. J Phys Chem A 2003, 107, 3733–3740.
32. Lazarou, Y. G.; Prosmitis, A. V.; Papadimitriou, V. C.; Papagiannakopoulos, P. J Phys Chem A 2001, 105, 6729–6742.
33. Perdew, J. P.; Chevary, J. A.; Vosko, S. H.; Jackson, K. A.; Pederson, M. R.; Singh, D. J.; Fiolhais, C. Phys Rev B 1992, 46, 6671–6687.
34. Papadimitriou, V. C.; Kambanis, K. G.; Lazarou, Y. G.; Papagiannakopoulos, P. J Phys Chem A 2004, 108, 2666–2674.
35. Curtiss, L. A.; Raghavachari, K.; Redfern, P. C.; Pople, J. A. J Chem Phys 1998, 109, 42–55.
36. McLean, A. D.; Chandler, G. S. J Chem Phys 1980, 72, 5639–5648.
37. Frisch, M. J.; Pople, J. A.; Binkley, J. S. J Chem Phys 1984, 80, 3265–3269.
38. Gill, P. M. W; Johnson, B. G; Pople, J. A.; Frisch, M. J. Chem Phys Lett 1992, 197, 499–505.
39. Dunning, T. H., Jr. J Chem Phys 1989, 90, 1007–1023.
40. Dunning, T. H., Jr.; Peterson, K. A.; Wilson, A. K. J Chem Phys 2001, 114, 9244–9253.
41. Woon, D.; Dunning, T. H., Jr. J Chem Phys 1993, 98, 1358–1371.
42. von Sonntag, C.; Schuchmann, H.-P. In Peroxyl Radicals in Aqueous Solutions in Peroxyl Radicals; Z. Alfassi (Ed.); Wiley: Chichester, UK, 1997; pp. 173–234.
43. Yurkova, I. L.; Schuchmann, H.-P.; von Sonntag, C. J Chem Soc, Perkin Trans 2 1999, 2049–2052.
44. Logager, T.; Holcman, J.; Sehested, K.; Pedersen, T. Inorg Chem 1992, 31, 3523–3529.
45. Balch, A. L.; Lamar, G. N.; Latosgrazynski, L.; Renner, M. W.; Thanabal, V. J Am Chem Soc 1985, 107, 3003–3007.
46. Laidler, K. J. Chemical Kinetics, 3rd ed.; Harper Collins: New York, 1987.
47. DeMore, W. B.; Sander, S. P.; Golden, D. M.; Hampson, R. F.; Kurylo, M. J.; Howard, C. J.; Ravishankara, A. R.; Kolb, C. E.; Molina, M. J. Chemical Kinetics and Photochemical Data for Use in Stratospheric; JPL Publication 97-4, 1997.
48. Chase, M. W. J. J Phys Chem Ref Data, Monograph 9, 1998, 1–1951.
49. NIST Standard Reference Database Number 69, February 2000 Release. Available at http://webbook.nist.gov/chemistry/.
50. Evans, M.; Polanyi, M. Trans Faraday Soc 1936, 32, 1333–1360.
51. Benson, S. W. The Foundations of Chemical Kinetics; McGraw-Hill: New York, 1982.
52. Donahue, N. M.; Clarke, J. S.; Anderson, J. G. J Phys Chem A 1998, 102, 3923–3933.
53. Donahue, N. M. J Phys Chem A 2001, 105, 1489–1497.
54. Vasil'ev, E. S.; Morozov, I. I.; Hack, W.; Hoyermann, K.; Hold, M.; Dorofeev, Y. I. Dokl Phys Chem 2001, 381, 293–297.
55. Wolke, R.; Sehili, A. M.; Simmel, M.; Knoth, O.; Tilgner, A.; Herrmann, H. Atmos Environ 2005, 39, 4375–4388.
56. CAPRAM's official Web site: http://projects.tropos.de/capram/
57. Wallington, T. J.; Dagaut, P.; Kurylo, M. J. J Phys Chem 1988, 92, 5024–5028.
58. Inoue, G.; Izumi, K.; Lozovoy, V. A. In Proceeding of the Third International Conference on Chemical Kinetics 1993, Gaithersburg, MD, pp. 182–183.